Noise-like pulse generation from a thulium-doped fiber laser using nonlinear polarization rotation with different net anomalous dispersion

Shuo Liu,[1] Fengping Yan,[1,*] Yang Li,[2] Luna Zhang,[1] Zhuoya Bai,[1] Hong Zhou,[3] and Yafei Hou[4]

[1]*Key Laboratory of All Optical Network & Advanced Telecommunication of EMC, Institute of Lightwave Technology, Beijing Jiaotong University, Beijing 100044, China*

[2]*Institute of Applied Physics and Computational Mathematics, Beijing 100094, China*

[3]*Department of Electronics, Information and Communication Engineering, Osaka Institute of Technology, 5-16-1 Omiya, Asahi-ku, Osaka 535-8585, Japan*

[4]*Graduate School of Information Science, Nara Institute of Science and Technology, 8916-5 Takayama, Ikoma Nara 630-0195, Japan*

**Corresponding author: fpyan@bjtu.edu.cn*

Received August 17, 2016; revised October 9, 2016; accepted October 11, 2016; posted October 27, 2016 (Doc. ID 273947); published November 28, 2016

A mode-locked thulium-doped fiber laser (TDFL) based on nonlinear polarization rotation (NPR) with different net anomalous dispersion is demonstrated. When the cavity dispersion is -1.425 ps^2, the noise-like (NL) pulse with coherence spike width of 406 fs and pulse energy of 12.342 nJ is generated at a center wavelength of 2003.2 nm with 3 dB spectral bandwidth of 23.20 nm. In the experimental period of 400 min, the 3 dB spectral bandwidth variation, the output power fluctuation, and the central wavelength shift are less than 0.06 nm, 0.04 dB, and 0.4 nm, respectively, indicating that the NPR-based TDFL operating in the NL regime holds good long-term stability.

OCIS codes: (140.3070) Infrared and far-infrared lasers; (140.3538) Lasers, pulsed; (320.7090) Ultrafast lasers.

http://dx.doi.org/10.1364/PRJ.4.000318

1. INTRODUCTION

The mode-locked thulium-doped fiber laser (TDFL) has gained increasing interest, revealing a number of applications in medicine, industry, and the military. It is well known that liquid water has strong absorption at the 2 μm band, and therefore it is more efficient to apply 2 μm ultrafast lasers to perform biological diagnostics or surgery [1]. Various approaches have been proposed to achieve mode-locked TDFL. A saturable absorber (SA) device is usually used inside the laser cavity, which plays an extremely important role in stabilizing mode-locked operation and shortening ultrafast pulses [2]. Besides, the nonlinear effects occurring in fibers are often utilized to alleviate the mode competition caused by the homogeneous gain broadening, like nonlinear polarization rotation (NPR), nonlinear amplifying loop mirror (NALM), and nonlinear optical loop mirror (NOLM).

The NPR effect is a very important and effective method to achieve mode-locked pulse operation, which has been widely used in mode-locked fiber lasers [3]. Instead of a polarization-dependent isolator, an NPR based mode-locked TDFL is demonstrated by using a 45° tilted fiber grating as an in-line polarizer to emit a 2.2 ps soliton pulse [4]. Moreover, the NPR technique could introduce the self-starting harmonic mode locking [5]. The different group delay dispersion in the laser cavity produces a different ultrafast pulse out. As for the different group delay dispersion in the laser cavity, a small-core and high numerical aperture fiber can provide normal dispersion [6], and the single-mode fiber (SMF) can provide anomalous dispersion [7].

A long-cavity mode-locked fiber laser can generate a low repetition rate and high energy pulse by using different lengths of all-wave fiber [8], highly nonlinear fiber [9], or SMF [10] to change the length of the cavity. The properties of noise-like (NL) pulses could also be controlled by changing the cavity [11]. Runge *et al.* reported on an experimental study of coherence and fluctuations in NL pulse fiber lasers [12]. The pulse generated in long-cavity mode-locked fiber laser not only suited convenient front-ends for chirped-pulse compression systems [13] but also could reduce the pump power required for supercontinuum generation [14]. There were some important works on NL pulse lasers in the 2 μm band. The mode-locked TDFLs based on NPR or NOLM could operate under two different regimes of solitary and NL pulses [15,16]. Based on the NPR, a 17.3 nJ NL pulse with 60.2 nm spectral bandwidth was obtained [17]. Based on NALM, TDFL generated a 460 fs NL pulse with pulse energy of 32.72 nJ [18]. An over 100 ps NL pulse with pulse energy of 1.27 nJ was enabled by using single-wall carbon nanotubes as the SA [19].

In this paper, NL pulse generation from the TDFL based on NPR with different net anomalous dispersion is first proposed in the 2 μm band. The NPR acts as a fast SA. By using additional SMFs with different lengths, the proposed lasers can achieve different ultrafast NL pulse output.

2. EXPERIMENTAL SETUP AND PRINCIPLE

The experimental setup of the proposed mode-locked TDFL is shown in Fig. 1. The gain spectrum centered at the ~2 μm band is provided by 5 m long commercial double-cladding thulium-doped fiber (TDF, CorActive) pumped by a 793 nm laser diode (LD) through a 793/2000 nm fiber combiner (FC). The NPR is performed by the combination of two polarization controllers (PCs) and a polarizer. The optical isolator is used to enforce unidirectional operation for the laser. A 90:10 fiber coupler is employed to extract 90% power from the laser cavity. The anomalous dispersion of the TDF and the SMF-28 are about –91 and –70.8 ps^2/km at the 2 μm band [20]. The pigtail fiber from the passive components is approximately 3.7 m in total, neglecting the length of the components themselves. For the purpose of the different cavity dispersion, we used additional SMFs with different lengths of 10, 20, 100, and 200 m corresponding to net dispersions of –1.425, –2.133, –7.797, and –14.877 ps^2, respectively. The operation principle of the NPR technique is shown in Fig. 1. By adjusting the PC2, the input lights possess various elliptical polarization states. With the SMF to provide the nonlinear phase shift, the lights with different elliptical polarization states propagate through the polarizer with different losses. Only one linearly polarized mode can propagate through the polarizer with low loss while the other orthogonal modes bear high loss.

We define θ as the angle between the polarization direction of the input light and the fast axis of the SMF, and β as the angle between the fast axes of the SMF and the polarizer. The transmission characteristic of the NPR can be obtained [21]:

$$T = \sin^2\theta\sin^2\beta + \cos^2\theta\cos^2\beta + \frac{1}{2}\sin(2\theta)\sin(2\beta)\cos(\Delta\phi_L + \Delta\phi_{NL}), \quad (1)$$

where $\Delta\phi_L$ and $\Delta\phi_{NL}$ are the linear and nonlinear phase differences, respectively. These phase terms are given by [22]

$$\Delta\phi_L = 2\pi\Delta nL/\lambda$$
$$\Delta\phi_{NL} = 2\pi n_2 PL\cos(2\theta)/\lambda A_{eff}, \quad (2)$$

where Δn is the refractive index difference between the fast axis and the slow axis of the SMF, L is the actual length of the SMF in the laser cavity, n_2 is the nonlinear refractive index, P is the instantaneous power of input lights, λ is the operating wavelength, and A_{eff} is the effective mode area. The NPR acts as a fast SA such that the higher intensity input light experiences lower loss. Thus, the high-intensity pulses can be transmitted while the low intensity pulses are highly reflected.

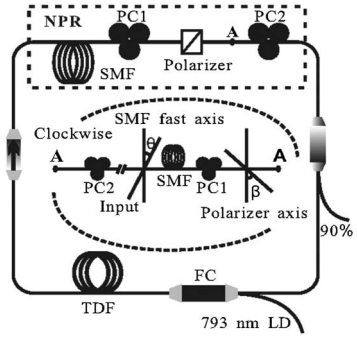

Fig. 1. Setup of the proposed mode-locked TDFL using the NPR.

The proposed NPR-based mode-locked TDFL operates in the NL regime. The NL pulse formation is affected by the NPR. By adjusting the PCs, the angles θ and β can be varied. By changing the length of the SMF, the $\Delta\phi_L$ and $\Delta\phi_{NL}$ can be changed. The $\Delta\phi_{NL}$ can be enhanced by improving the pump power.

3. EXPERIMENTAL RESULTS AND DISCUSSION

The spectrum was monitored by an optical spectrum analyzer (OSA; YOKOGAWA AQ6375). In case of optical damage, a 20 dB optical attenuator was used in front of the OSA input, which is not shown in Fig. 1. During the experiment, the proposed mode-locked TDFL started to operate at continuous wave after reaching the pump power of 1.172 W. When the pump power was increased to 1.756 W, the stable mode-locked solitary pulse was achieved by carefully adjusting the PCs. As the pump power increased to 2.18 W, the NPR-based TDFL was switched to a stable mode-locked NL regime by rotating the PCs. Figure 2 shows the spectra of the NL pulse with different SMF lengths; the pump power was fixed at 3.33 W. The mode-locked TDFL with different net anomalous dispersion generated broad and smooth spectra. The spectra characteristics are well consistent with the NL pulse laser. While the cavity dispersion varied from –1.425 to –14.877 ps^2, the 3 dB spectral bandwidth of the NL pulse ranged from 18.56 to 23.20 nm. It can be seen that the 3 dB spectral bandwidth of the NL pulse with 10 m SMF is the widest. The central wavelength and the 3 dB spectral bandwidth of the optical spectrum are 2003.2 and 23.20 nm; the optical signal-to-noise ratio (SNR) of the generated wavelength is as high as 39 dB for the 10 m SMF case as shown in Fig. 2(a).

In order to evaluate the stability of the NPR-based mode-locked TDFL with 10 m SMF, the measurements were carried out with an interval of 20 min, and the laser was maintained at the free running state during the measurements, as shown in Fig. 3. When the measuring time is 400 min, the 3 dB spectral bandwidth variation, the output power fluctuation, and the wavelength shift of the laser output are less than 0.06 nm, 0.04 dB, and 0.4 nm, respectively; the slight fluctuations of the laser output arise from the mode competition and hopping during the lasing process. These negligible variations proved that the proposed mode-locked TDFL could operate at a high wavelength and power-stable state.

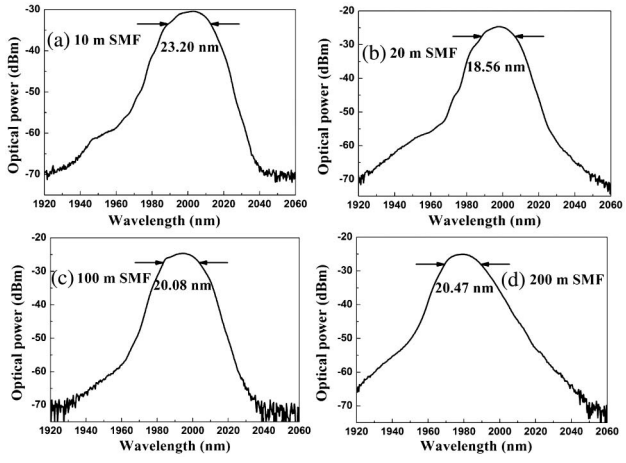

Fig. 2. Spectra of the NL pulse with different length of SMFs.

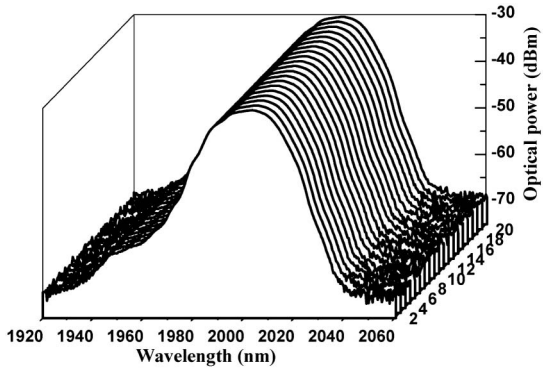

Fig. 3. Spectra of the NL pulse for 10 m SMF at 20 min intervals.

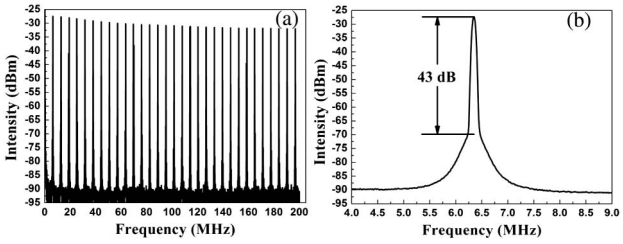

Fig. 4. RF spectra of NL pulse for 10 m SMF with scanning range of (a) 200 and (b) 5 MHz.

The radio frequency (RF) spectrum of the NL pulse is measured by an electrical spectrum analyzer (Agilent N9010A) from the detected signals of the 1 GHz photodetector (PD). Figure 4 shows the RF spectra of the NL pulse at the pump power level of 3.33 W for the 10 m SMF case. Figure 4(a) shows the RF spectrum of the NL pulse at a scanning range of 200 MHz with a frequency resolution of 20 kHz. The phases of various longitudinal modes are synchronized, and the phase difference between any neighboring modes is locked to a constant value, which confirms that the mode-locked TDFL can work steadily. The RF spectrum of the NL pulse at a scanning range of 5 MHz with a resolution bandwidth of 50 kHz is presented in Fig. 4(b). No sidebands can be observed within the frequency range, which indicates that the oscillator operates at the fundamental mode-locking regime. The measured repetition rate is 6.32 MHz, and the SNR of the fundamental frequency is up to 43 dB.

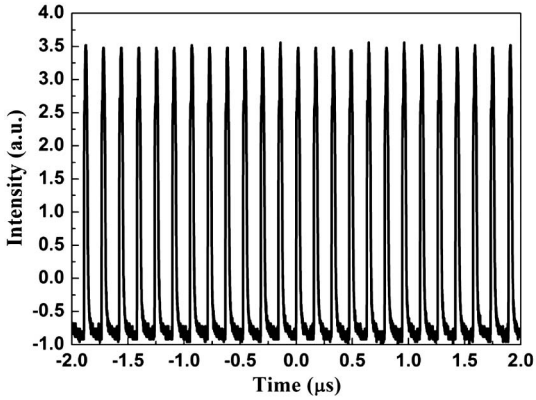

Fig. 5. Time-domain trace of the NL pulse with 10 m SMF.

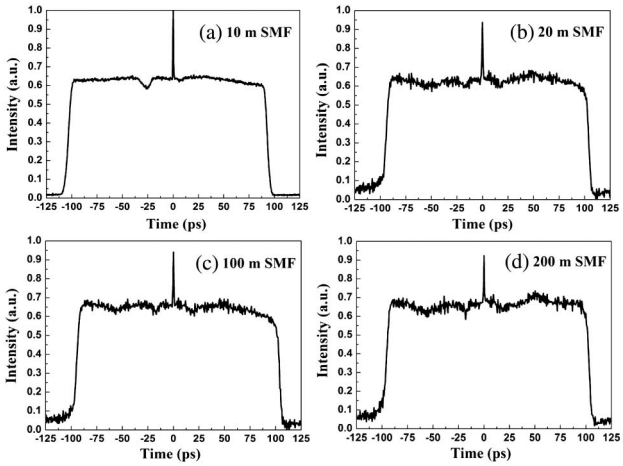

Fig. 6. Autocorrelation traces of the NL pulse for different length of SMFs with scanning range of 250 ps.

The repetition rate of the NL pulse could also be obtained from the time-domain traces of the proposed laser. The pump power was maintained at the 3.33 W level, and the detected signals from the PD were sent to a digital phosphor oscilloscope (Tektronix DPO3032). Figure 5 shows the measured time-domain signal from the oscilloscope. The calculated repetition rate of the NL pulse according to the time-domain trace is 6.32 MHz, which matches well with the laser cavity length.

The autocorrelation trace of the pulse is measured by an autocorrelator (Femtochrome, FR-103/XL). Figure 6 shows the autocorrelation traces of the NL pulse for different SMF lengths with a wide scanning range of 250 ps at the 3.33 W pump level. The autocorrelation traces show a coherence artifact on top of a background level, which is a classic signature of the NL pulse. All of this indicates the mode-locked TDFL using the NPR with different length of SMFs operates in the NL pulses state.

Figure 7 shows the autocorrelation traces of the NL pulse with different SMF lengths when the scanning range further reduces to 10 ps. The measured curves are fitted using a sech^2 pulse profile. It can be seen that the FWHMs of the NL pulse are 0.626, 0.996, 0.825, and 0.739 ps with different SMF lengths, which corresponds to the coherence spike widths of

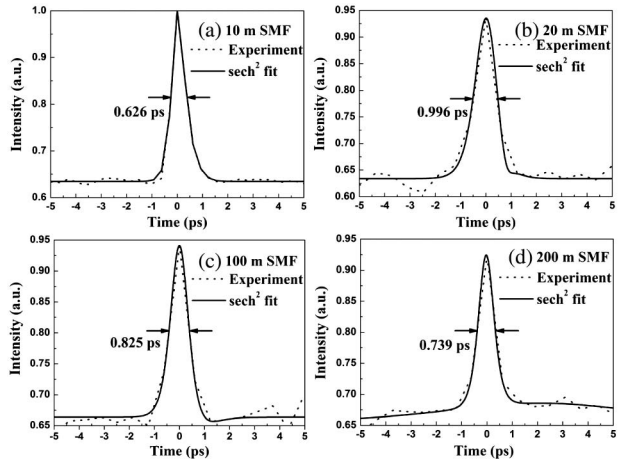

Fig. 7. Autocorrelation traces of the NL pulse for different length of SMFs with scanning range of 10 ps.

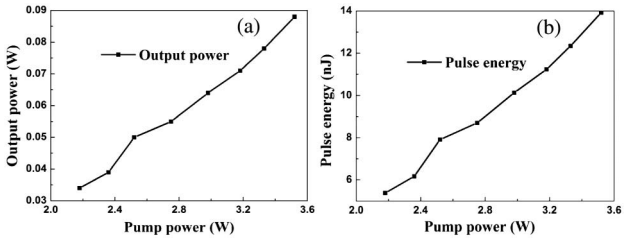

Fig. 8. Output power and the NL pulse energy versus the pump power with 10 m SMF.

406, 645, 535, and 479 fs. It is revealed that the coherence spike width is 406 fs, which correspond to the total net dispersion of −1.425 ps^2 in the laser cavity.

The output power is measured by a thermopile power detector. Figure 8 shows the output power and the pulse energy of the NL pulse versus the pump power with 10 m SMF. It can be seen that the output power of the NL pulse increases linearly with increasing pump power. At the 3.33 W pump power, the NL pulse has an output power of 0.078 W. The slope efficiency of 3.8% is observed for stable mode-locked TDFL. When the repetition rate is 6.32 MHz, the NL pulse energy is evaluated to be 12.342 nJ under 3.33 W pump power. Compared with the SA-based mode-locked TDFL [23], the nonlinear effect based NPR structure can achieve higher energy owing to the higher damage threshold without the real SA. In order to obtain high pulse energy, the TDFL requires only increasing the pump power.

4. CONCLUSION

The generation of NL pulse in TDFL based on NPR with different net anomalous dispersion is first proposed and realized in the 2 μm band. The proposed mode-locked TDFL can produce stable NL pulse for at least 400 min. When the cavity dispersion is −1.425 ps^2, the NL pulse centered at 2003.2 nm with 3 dB spectral bandwidth of 23.20 nm is generated at the repetition rate of 6.32 MHz with a coherence spike width of 406 fs and pulse energy of 12.342 nJ.

Funding. Fundamental Research Funds for the Central Universities (2016YJS034).

REFERENCES

1. R. Szlauer, R. Götschl, A. Razmaria, L. Paras, and N. T. Schmeller, "Endoscopic vaporesection of the prostate using the continuous-wave 2-μm thulium laser: outcome and demonstration of the surgical technique," Eur. Urol. **55**, 368–375 (2009).
2. S. Azooz, F. Ahmad, H. Ahmad, S. Harun, B. Hamida, S. Khan, A. Halder, M. C. Paul, M. Pal, and S. K. Bhadra, "Mode-locked 2 μm fiber laser with a multi-walled carbon nanotube as a saturable absorber," Chin. Opt. Lett. **13**, 030602 (2015).
3. Z. C. Tiu, S. J. Tan, H. Ahmad, and S. W. Harun, "Dark pulse emission in nonlinear polarization rotation-based multiwavelength mode-locked erbium-doped fiber laser," Chin. Opt. Lett. **12**, 113202 (2014).
4. J. Li, Z. Yan, Z. Sun, H. Luo, Y. He, Z. Li, Y. Liu, and L. Zhang, "Thulium-doped all-fiber mode-locked laser based on NPR and 45°-tilted fiber grating," Opt. Express **22**, 31020–31028 (2014).
5. X. Wang, P. Zhou, X. Wang, H. Xiao, and Z. Liu, "Pulse bundles and passive harmonic mode-locked pulses in Tm-doped fiber laser based on nonlinear polarization rotation," Opt. Express **22**, 6147–6153 (2014).
6. F. Haxsen, D. Wandt, U. Morgner, J. Neumann, and D. Kracht, "Monotonically chirped pulse evolution in an ultrashort pulse thulium-doped fiber laser," Opt. Lett. **37**, 1014–1016 (2012).
7. X. Yang, Y. Chen, C. Zhao, and H. Zhang, "Pulse dynamics controlled by saturable absorber in a dispersion-managed normal dispersion Tm-doped mode-locked fiber laser," Chin. Opt. Lett. **12**, 031405 (2014).
8. S. Kobtsev, S. Kukarin, and Y. Fedotov, "Ultra-low repetition rate mode-locked fiber laser with high-energy pulses," Opt. Express **16**, 21936–21941 (2008).
9. R. I. Woodward, E. J. R. Kelleher, D. Popa, T. Hasan, F. Bonaccorso, A. C. Ferrari, S. V. Popov, and J. R. Taylor, "Scalar nanosecond pulse generation in a nanotube mode-locked environmentally stable fiber laser," IEEE Photon. Technol. Lett. **26**, 1672–1675 (2014).
10. M. Erkintalo, C. Aguergaray, A. Runge, and N. G. R. Broderick, "Environmentally stable all-PM all-fiber giant chirp oscillator," Opt. Express **20**, 22669–22674 (2012).
11. M. Horowitz and Y. Silberberg, "Control of noiselike pulse generation in erbium-doped fiber lasers," IEEE Photon. Technol. Lett. **10**, 1389–1391 (1998).
12. A. F. J. Runge, C. Aguergaray, N. G. R. Broderick, and M. Erkintalo, "Coherence and shot-to-shot spectral fluctuations in noise-like ultrafast fiber lasers," Opt. Lett. **38**, 4327–4330 (2013).
13. R. I. Woodward, E. J. R. Kelleher, T. H. Runcorn, S. Loranger, D. Popa, V. J. Wittwer, A. C. Ferrari, S. V. Popov, R. Kashyap, and J. R. Taylor, "Fiber grating compression of giant-chirped nanosecond pulses from an ultra-long nanotube mode-locked fiber laser," Opt. Lett. **40**, 387–390 (2015).
14. A. Zaytsev, C.-H. Lin, Y.-J. You, C.-C. Chung, C.-L. Wang, and C.-L. Pan, "Supercontinuum generation by noise-like pulses transmitted through normally dispersive standard single-mode fibers," Opt. Express **21**, 16056–16062 (2013).
15. Q. Wang, T. Chen, B. Zhang, A. P. Heberle, and K. P. Chen, "All-fiber passively mode-locked thulium-doped fiber ring oscillator operated at solitary and noiselike modes," Opt. Lett. **36**, 3750–3752 (2011).
16. J. Li, Z. Zhang, Z. Sun, H. Luo, Y. Liu, Z. Yan, C. Mou, L. Zhang, and S. K. Turitsyn, "All-fiber passively mode-locked Tm-doped NOLM-based oscillator operating at 2-μm in both soliton and noisy-pulse regimes," Opt. Express **22**, 7875–7882 (2014).
17. H. Xin, L. Aiping, Y. Qi, Y. Tong, Y. Xiaozhi, X. Shanhui, Q. Qi, C. Dongdan, L. Zhichao, X. Wencheng, and Y. Zhongmin, "60 nm bandwidth, 17 nJ noiselike pulse generation from a thulium-doped fiber ring laser," Appl. Phys. Express **6**, 112702 (2013).
18. L. Shuo, Y. Feng-Ping, Z. Lu-Na, H. Wen-Guo, B. Zhuo-Ya, and Z. Hong, "Noise-like femtosecond pulse in passively mode-locked Tm-doped NALM-based oscillator with small net anomalous dispersion," J. Opt. **18**, 015508 (2016).
19. Q. Wang, T. Chen, M. Li, B. Zhang, Y. Lu, and K. P. Chen, "All-fiber ultrafast thulium-doped fiber ring laser with dissipative soliton and noise-like output in normal dispersion by single-wall carbon nanotubes," Appl. Phys. Lett. **103**, 011103 (2013).
20. R. Kadel and B. R. Washburn, "All-fiber passively mode-locked thulium/holmium laser with two center wavelengths," Appl. Opt. **51**, 6465–6470 (2012).
21. S. X. Liu, C. H. Wang, X. J. Zhu, C. X. Bu, and G. J. Zhang, "Arbitrarily switchable multi-wavelength Yb-doped fiber lasers with phase-shifted long-period fiber grating," Laser Phys. **22**, 1260–1264 (2012).
22. Z. Yan, X. Li, Y. Tang, P. P. Shum, X. Yu, Y. Zhang, and Q. J. Wang, "Tunable and switchable dual-wavelength Tm-doped mode-locked fiber laser by nonlinear polarization evolution," Opt. Express **23**, 4369–4376 (2015).
23. G. Sobon, J. Sotor, A. Przewolka, I. Pasternak, W. Strupinski, and K. Abramski, "Amplification of noise-like pulses generated from a graphene-based Tm-doped all-fiber laser," Opt. Express **24**, 20359–20364 (2016).